

Foundations of Quantum Error Correction

Master QLMN - Experimental quantum computing

François-Marie Le Régent

francois-marie.le-regent@pasqal.com

Pasqal

February 11, 2026

Table of contents

- Quiz: Exponential Suppression of Errors
- Classical Error Correction
- Quantum Repetition Code
- Shor Code
- The Stabilizer Formalism
- Surface Code
- Detectors and Decoding
- Threshold Theorem
- Fault-Tolerant Circuit Design
- Logical Gates

Master QLMN - Experimental quantum computing

Program

- Introduction and overview: qubits, gates, circuits and errors... 
- **Module 1: Hardware**
 - Qubits based on atoms and ions. 
 - Qubits based on superconducting circuits. 
 - Other qubits: photons, electron spins & NMR. 
- **Module 2: Algorithms and their experimental implementations**
 - Quantum algorithms 1: Shor's algorithm. 
 - Quantum algorithms 2: Grover, QFT, QPE & Resource Estimates. 
- **Module 3: Quantum error correction**
 - **Quantum error correction and description of codes.** 
 - Construction of a fault-tolerant architecture.

Quiz: Exponential Suppression of Errors

Q1: Code Implementation¹

Which quantum error correction code structure was primarily implemented to demonstrate the exponential suppression of errors in this experiment?

(i) A

A 2D surface code measuring both X and Z stabilizers simultaneously to correct all errors.

(i) B

A 1D repetition code embedded in a 2D grid, configured separately for either bit-flip or phase-flip protection.

(i) C

A Shor code encoding 1 logical qubit into 9 physical qubits.

(i) D

A bosonic cat code using superconducting cavities.

1. Chen et al. (2021)

Q1: Solution

Which quantum error correction code structure was primarily implemented to demonstrate the exponential suppression of errors in this experiment?

i A

A 2D surface code measuring both X and Z stabilizers simultaneously to correct all errors.

i B

A 1D repetition code embedded in a 2D grid, configured separately for either bit-flip or phase-flip protection.

i C

A Shor code encoding 1 logical qubit into 9 physical qubits.

i D

A bosonic cat code using superconducting cavities.



Correct Answer: B

- The experiment implemented a **1D repetition code** embedded in the 2D Sycamore chip grid.
- The code was configured separately for bit-flip protection (using $Z_i Z_{i+1}$ stabilizers) or phase-flip protection (using $X_i X_{i+1}$ stabilizers), but not both simultaneously.

Q2: Logical Error Scaling

According to the experimental results, how does the logical error probability per round (ϵ_L) scale with the code distance d ?

i A

Linearly: $\epsilon_L \propto 1/d$

i B

Quadratically: $\epsilon_L \propto 1/d^2$

i C

Exponentially: $\epsilon_L \propto \Lambda^{-d/2}$ where Λ is the error suppression factor.

i D

The logical error rate remained constant as d increased due to correlated noise.

Q2: Solution

According to the experimental results, how does the logical error probability per round (ϵ_L) scale with the code distance d ?

i A

Linearly: $\epsilon_L \propto 1/d$

i B

Quadratically: $\epsilon_L \propto 1/d^2$

i C

Exponentially: $\epsilon_L \propto \Lambda^{-d/2}$ where Λ is the error suppression factor.

i D

The logical error rate remained constant as d increased due to correlated noise.

💡 Correct Answer: C

- The main result is the **exponential suppression** of logical errors with code distance.
- $\Lambda > 1$ means each additional pair of qubits suppresses the error by a constant factor, demonstrating below-threshold operation.

Q3: Experimental Parameters

Which of the following correctly describe the scale of the repetition code experiments performed?

i A

The code distances ranged from $d = 3$ to $d = 11$.

i C

The experiment was limited to $d = 3$ due to chip size constraints.

i B

The largest code used 21 superconducting qubits (11 data qubits, 10 measure qubits).

i D

The logical error suppression was shown to be stable over 50 rounds of error correction.

Q3: Solution

Which of the following correctly describe the scale of the repetition code experiments performed?

i A

The code distances ranged from $d = 3$ to $d = 11$.

i B

The largest code used 21 superconducting qubits (11 data qubits, 10 measure qubits).

i C

The experiment was limited to $d = 3$ due to chip size constraints.

i D

The logical error suppression was shown to be stable over 50 rounds of error correction.

💡 Correct Answers: A, B, D

- The experiment demonstrated codes from $d = 3$ to $d = 11$ using up to 21 qubits, and showed stable suppression over 50 rounds.
- The Sycamore chip had sufficient qubits to go well beyond $d = 3$.

Q4: Error Handling Configuration

How did the experiment address the distinction between bit-flip and phase-flip errors?

i A

A single surface code patch corrected both error types concurrently.

i B

The “Phase-Flip Code” used $X_i X_{i+1}$ stabilizers to detect Z errors.

i C

The “Bit-Flip Code” used $Z_i Z_{i+1}$ stabilizers to detect X errors.

i D

Phase-flip errors were found to be negligible compared to bit-flip errors.

Q4: Solution

How did the experiment address the distinction between bit-flip and phase-flip errors?

i A

A single surface code patch corrected both error types concurrently.

i B

The “Phase-Flip Code” used $X_i X_{i+1}$ stabilizers to detect Z errors.

i C

The “Bit-Flip Code” used $Z_i Z_{i+1}$ stabilizers to detect X errors.

i D

Phase-flip errors were found to be negligible compared to bit-flip errors.

💡 Correct Answers: B, C

- The experiment ran **two separate configurations**.
- The bit-flip code measured $Z_i Z_{i+1}$ parity to catch X errors, while the phase-flip code measured $X_i X_{i+1}$ parity to catch Z errors.
- Each configuration protects against only one error type at a time.

Q5: Physical Error Model

What conclusion did the authors reach regarding the physical error mechanisms in the device?

i A

The errors were dominated by non-local cosmic ray events that destroyed the code immediately.

i B

The device performance was well-described by a simple uncorrelated depolarizing error model.

i C

T_1 relaxation was the sole limiting factor for both bit and phase codes.

i D

Correlated errors were significant enough to prevent any error suppression as distance increased.

Q5: Solution

What conclusion did the authors reach regarding the physical error mechanisms in the device?

i A

The errors were dominated by non-local cosmic ray events that destroyed the code immediately.

i B

The device performance was well-described by a simple uncorrelated depolarizing error model.

i C

T_1 relaxation was the sole limiting factor for both bit and phase codes.

i D

Correlated errors were significant enough to prevent any error suppression as distance increased.



Correct Answer: B

- The device noise was well-modeled by **simple uncorrelated Pauli errors**, which is why the exponential suppression with distance was observed.
- Correlated errors were present but subdominant.

Classical Error Correction

The Repetition Code

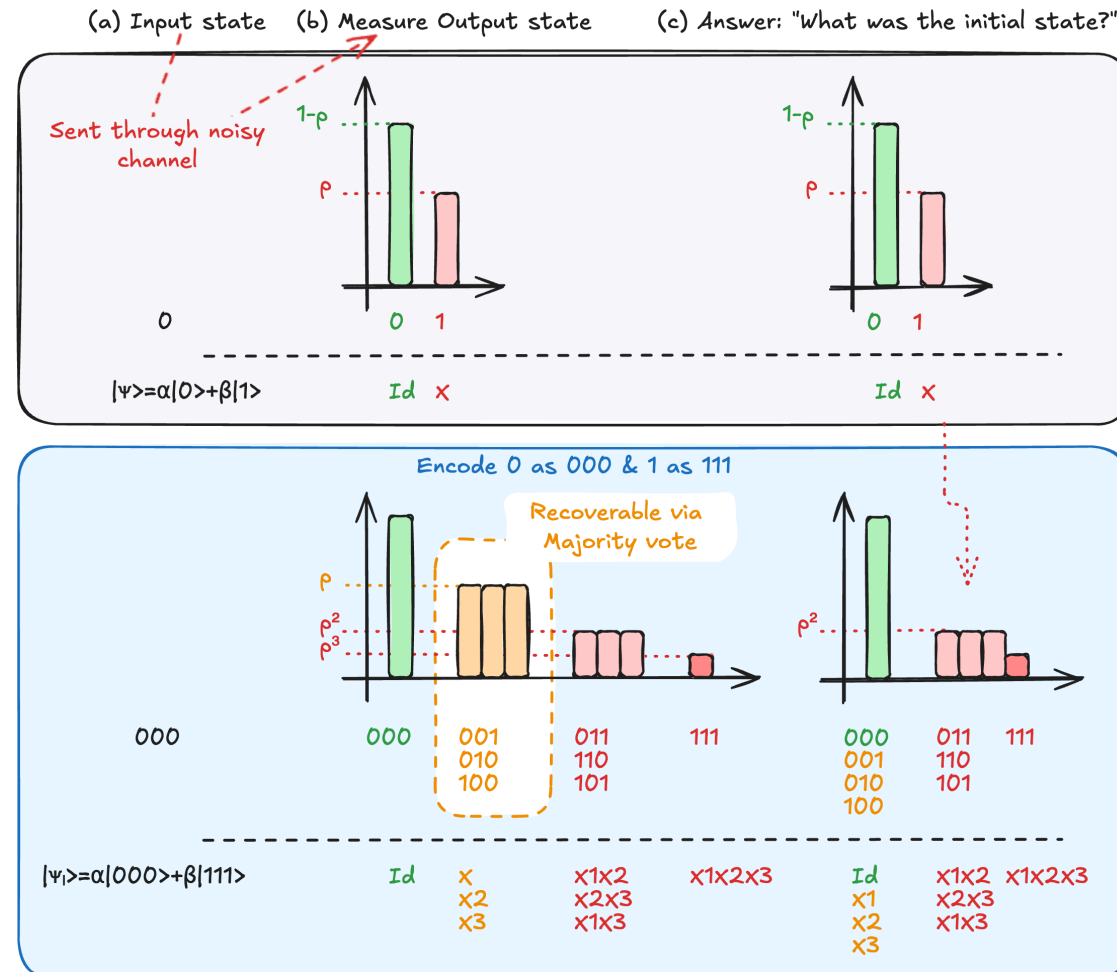


Figure 1: Error suppression in the 3-qubit repetition code: comparison of error probabilities between an unencoded single qubit (top) and a logical qubit encoded as $|0\rangle_L = |000\rangle$ (bottom).

Hamming Code: Parity and the Price of Information

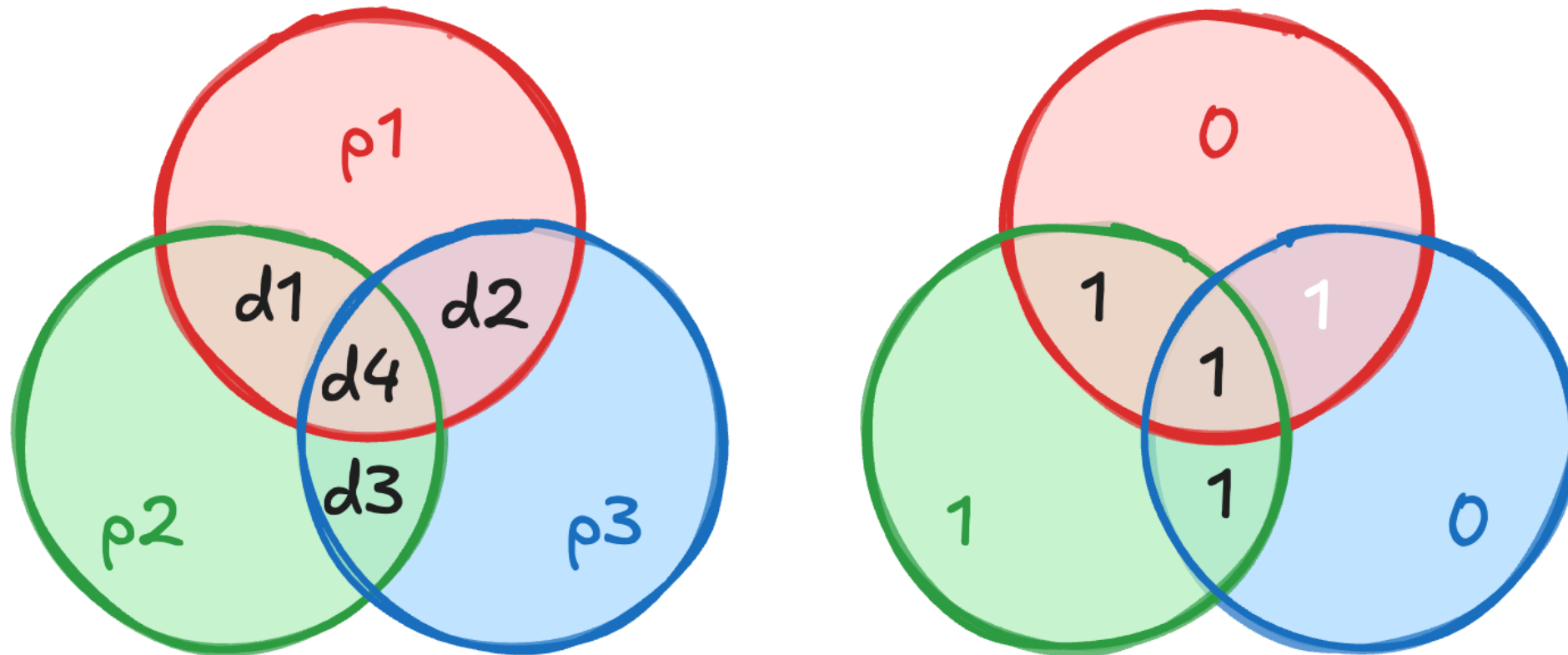


Figure 2: Venn diagram representation of the Hamming(7,4) code. Data bits sit at the intersections of three circles, with parity bits controlling each circle.

Quantum Repetition Code

Parity Measurement Circuit

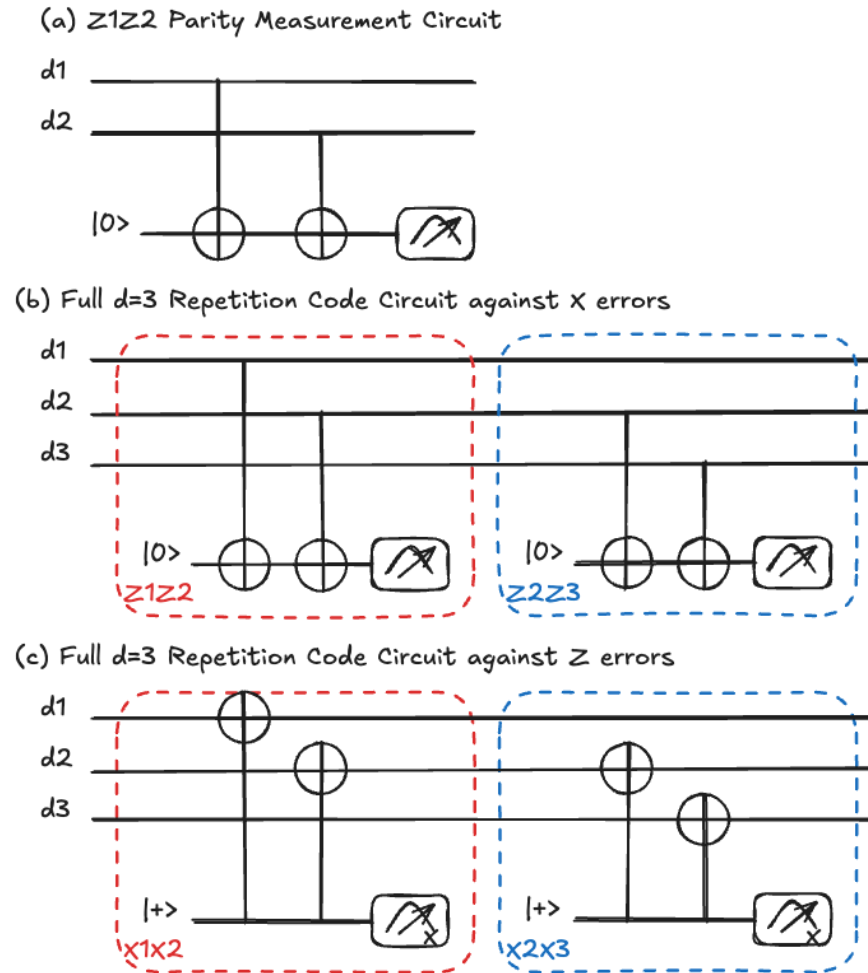
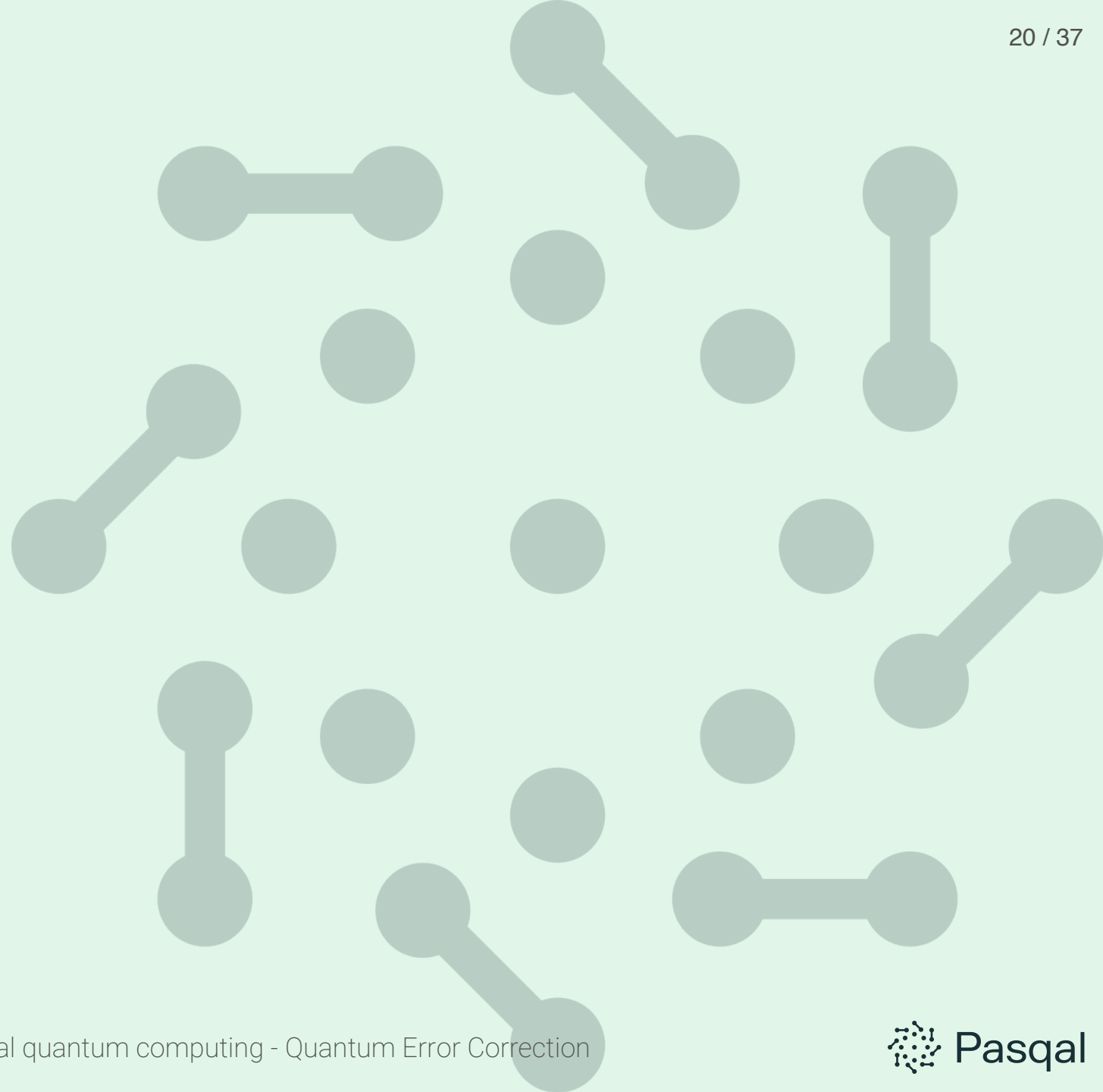


Figure 3: **a** Circuit for a single parity measurement. **b** Full syndrome extraction for the 3-qubit bit-flip code. **c** Full syndrome extraction for the 3-qubit phase-flip code.

Shor Code



Shor Code: Construction

Hierarchical protection against all single-qubit errors

$$|0\rangle_L = \frac{(|000\rangle + |111\rangle) \otimes (|000\rangle + |111\rangle) \otimes (|000\rangle + |111\rangle)}{2\sqrt{2}}$$

$$|1\rangle_L = \frac{(|000\rangle - |111\rangle) \otimes (|000\rangle - |111\rangle) \otimes (|000\rangle - |111\rangle)}{2\sqrt{2}}$$

Intuition

- **Inner blocks** (sets of 3 qubits): protect against **bit-flips**
- **Outer structure** (relative signs between blocks): protects against **phase-flips**

Shor Code: Encoding Circuit

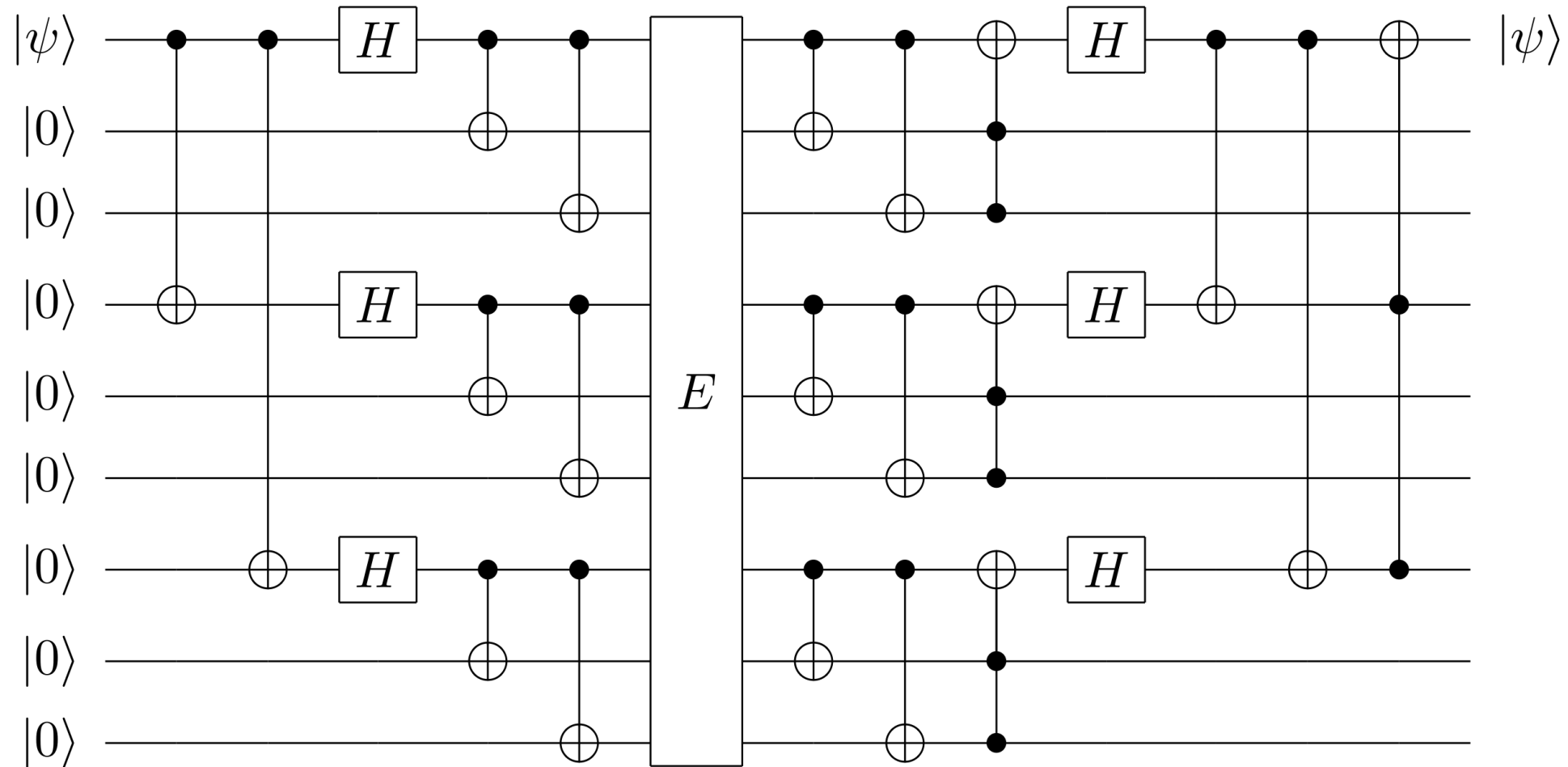


Figure 4: Circuit diagram for the 9-qubit Shor code encoding process.

The Stabilizer Formalism

General Stabilizer Measurement Circuit

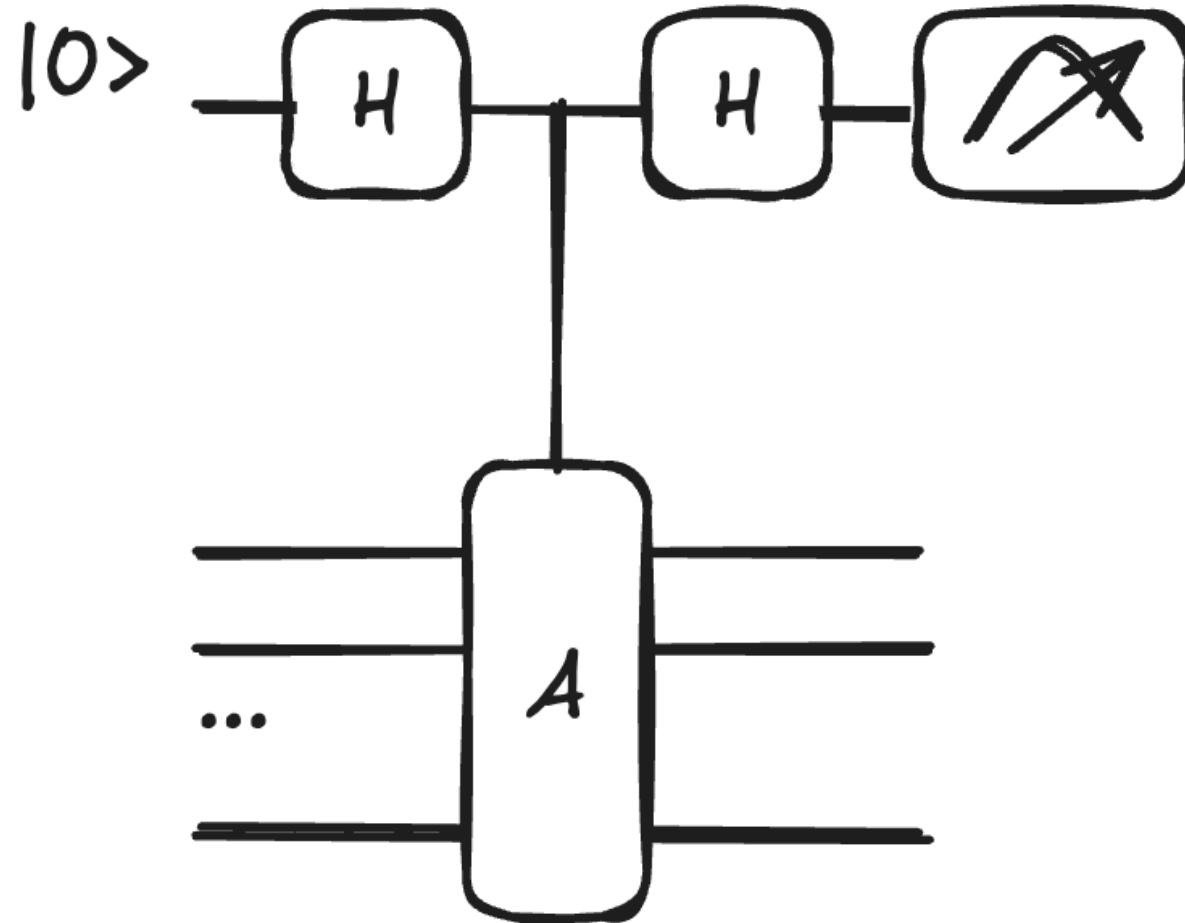


Figure 5: General circuit for measuring a stabilizer A using an ancilla qubit with Hadamard gates and a controlled- A operation.

Surface Code

Surface Code Lattice

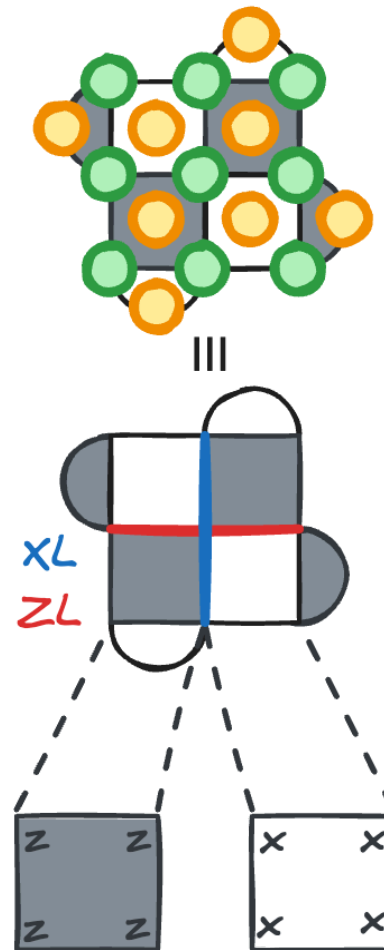


Figure 6: The surface code lattice: data qubits (green) on vertices, ancilla qubits (orange) in tile centers. Boundary-to-boundary products define logical operators Z_L (red) and X_L (blue).

Constructing $|0\rangle_L$ of the Surface Code

Start from $|0\dots 0\rangle$ and project into the stabilizer subspace

Each X -stabilizer projector $P = \frac{1}{2}(\mathbb{I} + X_a)$ creates entanglement¹:

💡 Full expression

$$\begin{aligned}
 |0_L\rangle = & |000000000\rangle + (-1)^d |000000110\rangle \\
 & + (-1)^a |011000000\rangle + (-1)^{a+d} |011000110\rangle \\
 & + (-1)^b |110110000\rangle + (-1)^{b+d} |110110110\rangle \\
 & + (-1)^{a+b} |101110000\rangle + (-1)^{a+b+d} |101110110\rangle \\
 & + (-1)^c |000011011\rangle + (-1)^{c+d} |000011101\rangle \\
 & + (-1)^{a+c} |011011011\rangle + (-1)^{a+c+d} |011011101\rangle \\
 & + (-1)^{b+c} |110101011\rangle + (-1)^{b+c+d} |110101101\rangle \\
 & + (-1)^{a+b+c} |101101011\rangle + (-1)^{a+b+c+d} |101101101\rangle
 \end{aligned}$$

1. where a, \dots, d represent the values of each X plaquette measurement.

Detectors and Decoding

The Spacetime Detection Graph

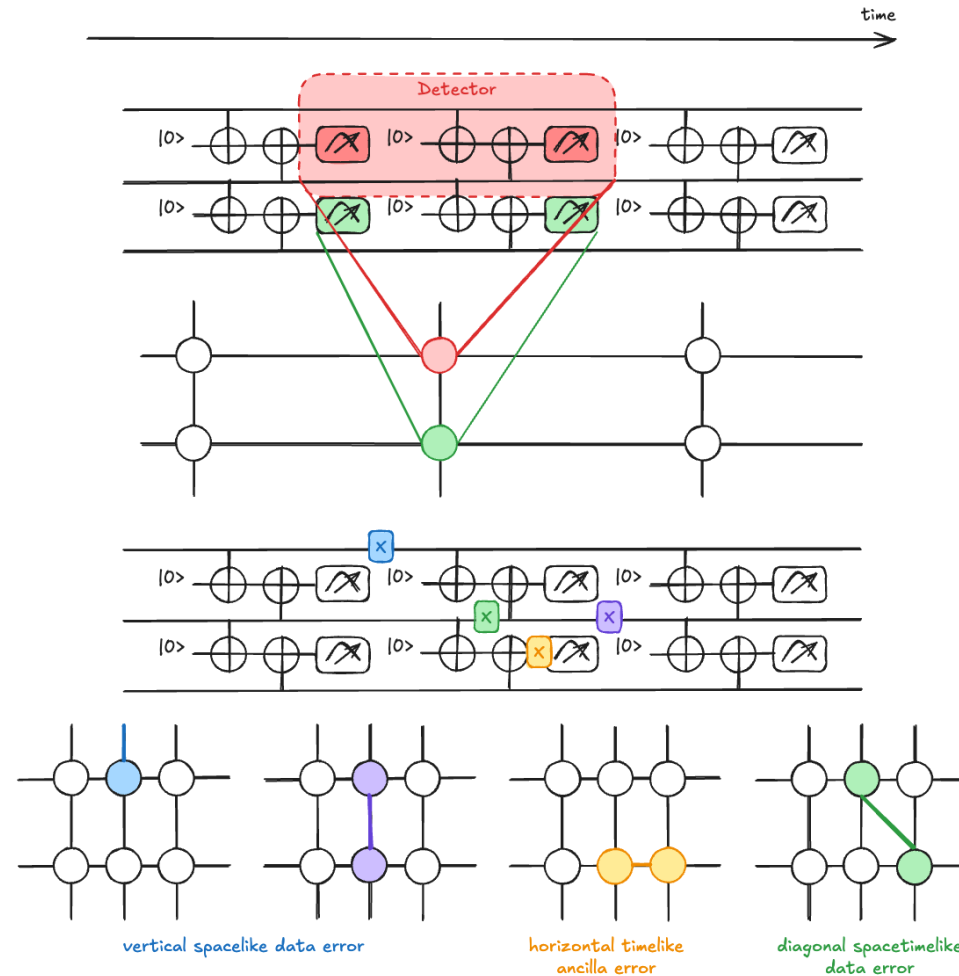


Figure 7: Spacetime detection graph for the repetition code. Nodes are detector events, horizontal edges are data errors, vertical edges are measurement errors, diagonal edges are errors between CNOTs.

Threshold Theorem

The Threshold Plot

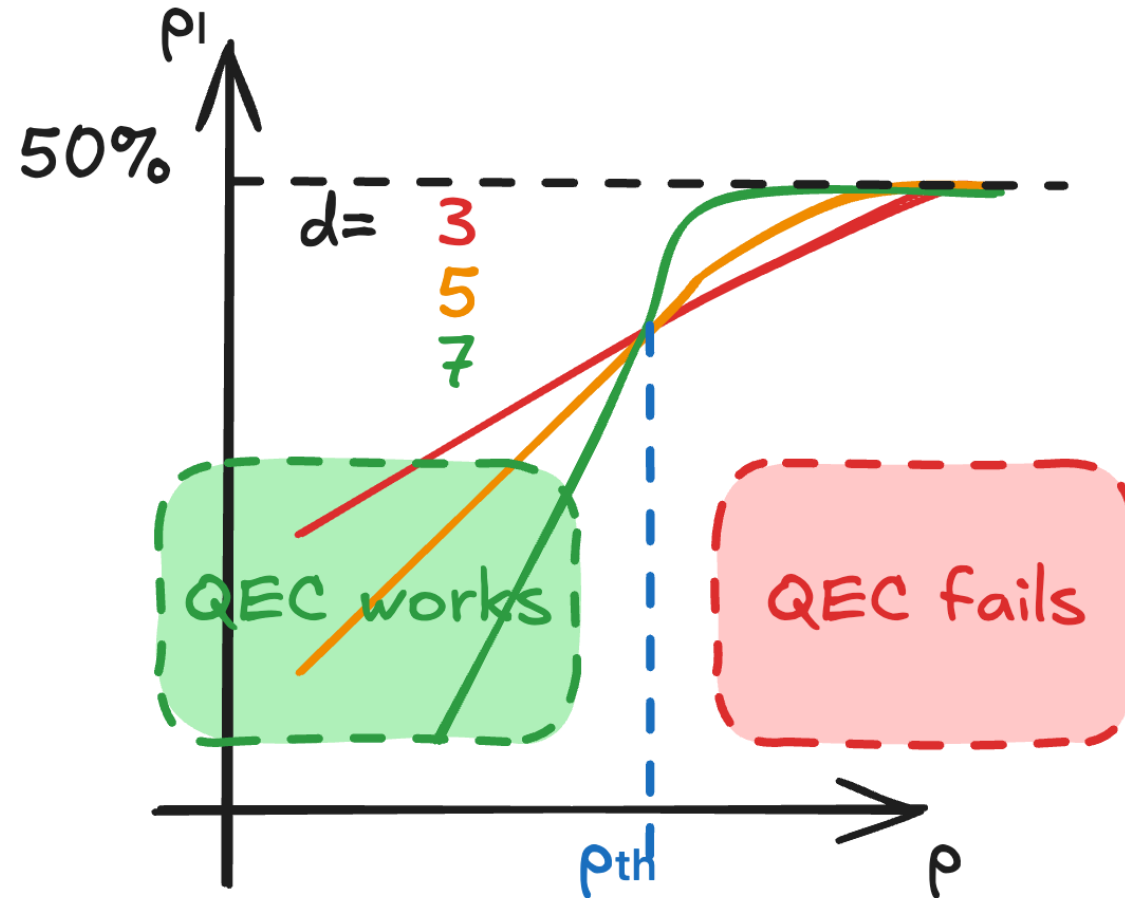


Figure 8: Threshold plot: logical error rate P_L vs physical error rate p for different code distances. The curves cross at the threshold p_{th} .

Fault-Tolerant Circuit Design

Gate Ordering for Fault Tolerance

Hook Errors

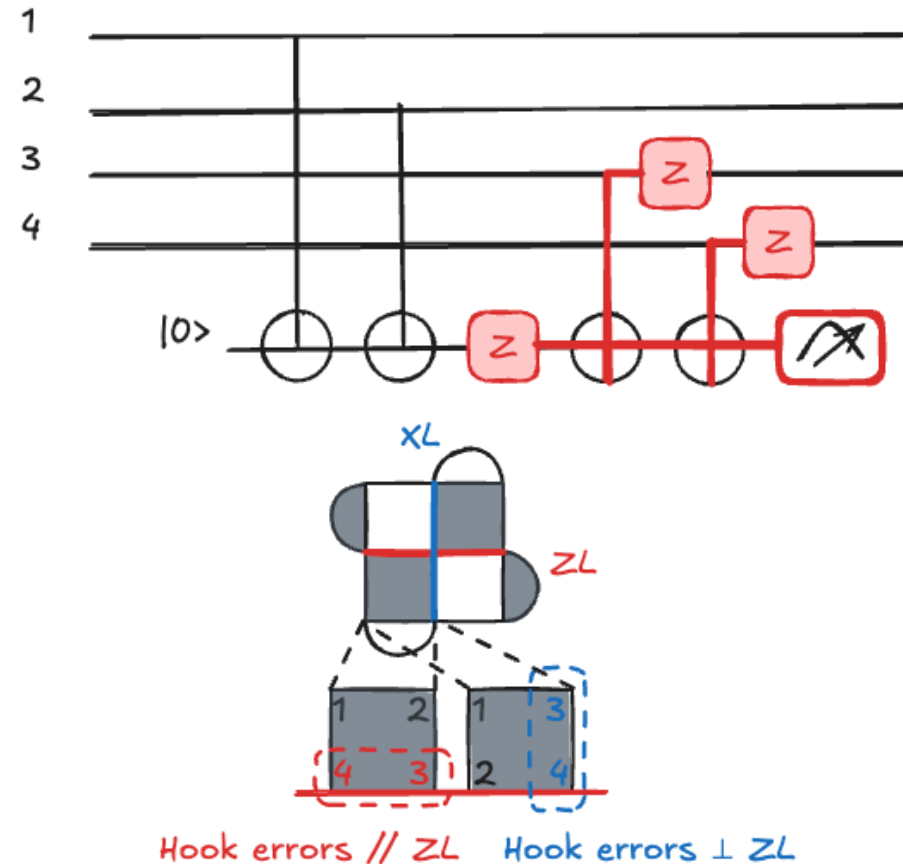


Figure 9: Comparison of CNOT ordering for a Z stabilizer to ensure fault tolerance. The last two qubits touched must propagate errors perpendicular to the logical Z_L operator.

Logical Gates

T Gate via Magic State Teleportation

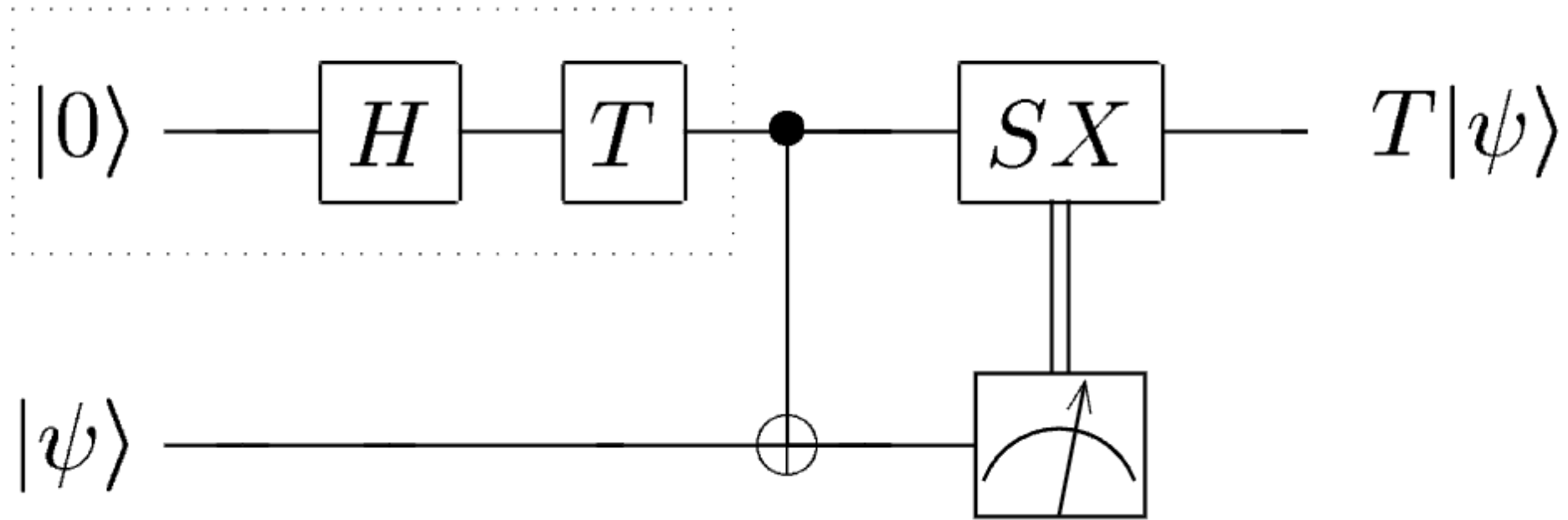


Figure 10: Circuit diagram for T-gate teleportation using a magic state $|\phi\rangle = T|+\rangle$ and a corrective S gate.

Thank you for your attention!

References

Chen, Zijun, Kevin J. Satzinger, Juan Atalaya, Alexander N. Korotkov, Andrew Dunsworth, Daniel Sank, Chris Quintana, et al. 2021. “Exponential Suppression of Bit or Phase Errors with Cyclic Error Correction.” *Nature* 595 (7867): 383–87. <https://doi.org/10.1038/s41586-021-03588-y>.